Syntheses and Characterization of Poly(phenylene sulfide)–Poly(ether sulfone) Block Copolymers

LI KUANG, QIXIAN WU, and YONGRONG CHEN*

Institute of Materials Science & Technology, Sichuan University, Chengdu, Sichuan 610064, People's Republic of China

SYNOPSIS

Poly(phenylene sulfide)–poly(ether sulfone) (PPS–PES) block copolymers were synthesized by polycondensation of chloro-terminated PPS oligomers and hydroxylic-terminated PES oligomers at atmospheric pressure. The structure and compositions of PPS–PES block copolymers were analyzed quantitatively by FTIR spectroscopy. It was found that the contents of PES in copolymers increase with the amount of PES in the added materials; however, the quantities of PES contents in copolymers are lower than its quantities in the added materials. The solubility, crystallization behavior, and thermal properties of PPS–PES block copolymers were studied through a solubility test, X-ray diffraction, DSC, and TGA. It was primarily proved that the copolymers have better solubility, lower crystallinity, and higher glass transition (T_g) than those of PPS. The nonisothermal crystallization kinetics and thermal decomposition kinetics of block copolymers were also studied; furthermore, the crystallization kinetic parameters and the activation energy of thermal decomposition were calculated. © 1996 John Wiley & Sons, Inc.

INTRODUCTION

Poly(phenylene sulfide) (PPS) is a versatile high-performance engineering plastic having prominent heat resistance, chemical resistance, good mechanical properties, and rigidity. However, the resin has insufficient toughness and is brittle, which limits its application. In recent years, a great effort has been made to improve the above properties; hence, blending and block copolymerization are necessary.[1-11]

Poly(ether sulfone) (PES) is an amorphous thermoplastic resin that possesses good heat resistance and toughness. So, the making of the PPS–PES block copolymer is an important way to improve the toughness and impact strength of PPS resin.

Although there are patents on the syntheses of the PPS–PES block copolymer from mercapto-terminated PPS oligomers and chloro-terminated PES oligomers,[4,5] the other method used by chloro-terminated PPS oligomers and hydroxylic-terminated PES oligomers has not been reported yet, and the fundamental research work on the PPS–PES block copolymer has not been sufficient. In this article, the work on syntheses and characterization of the above copolymer is reported.

EXPERIMENTAL

Materials

Hydroxylic-terminated PES oligomers were offered by the Chemistry Department of Jilin University, and chloro-terminated PPS oligomers were synthesized using endcapping by adding a monomer in the laboratory.[12,13] Dimethylacetamide (DMA), dimethylformamide (DMF), *n*-methyl-2-pyrrolidone (NMP), and hexamethylphosphoric triamide (HMPT) were distilled under reduced pressure prior to use. *m*-Cresol, phenol, 1,1,2,2-tetrachloroethane, and α-chloronaphthalene were used without further purification.

* To whom correspondence should be addressed.

Journal of Applied Polymer Science, Vol. 61, 1607–1614 (1996)
 CCC 0021-8995/96/091607-08

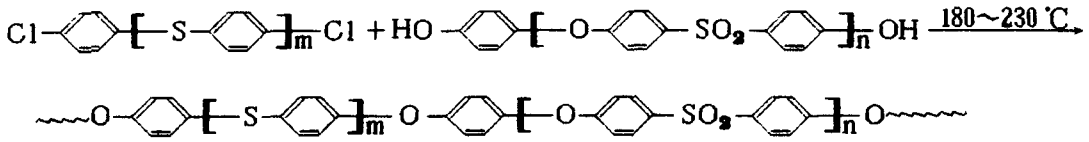

Scheme I A simple reaction path for the PPS and PES copolymerization.

Synthesis of Block Copolymers

The PPS–PES block copolymers were prepared using PPS oligomers with chloro-terminal groups and PES oligomers with hydroxylic-terminal groups in HMPT at atmospheric pressure (see Scheme I).

A 250 mL three-necked flask equipped with a mechanical stirrer, a thermometer, and a condenser was charged with 100 mL HMPT, 2 g NaOH, 10 g PPS oligomers, and 10 g PES oligomers. The mixture was reacted while stirring at 180°C for 1 h and then at 230°C for 3 h. After the reaction vessel was cooled to about 140°C, the yellowish white contents were poured into hot water, then subsequently filtered and washed with hot water many times to remove solvent and trapped salts. The resulting cake was dried at 120°C for 5 h to obtain 7.6 g of a grayish white polymer powder. In a Soxhlet extractor, the product was purified by extracting PPS oligomers with toluene, PES oligomers with chloroform, and inorganic impurities with deionized water and acetone. Then, the product was dried in a vacuum over 8 h and the PPS–PES block copolymer was obtained.

Characterization

IR Spectroscopy Analysis

Infrared data were recorded on a Nicolet Model 170SX Fourier transform infrared spectrometer.

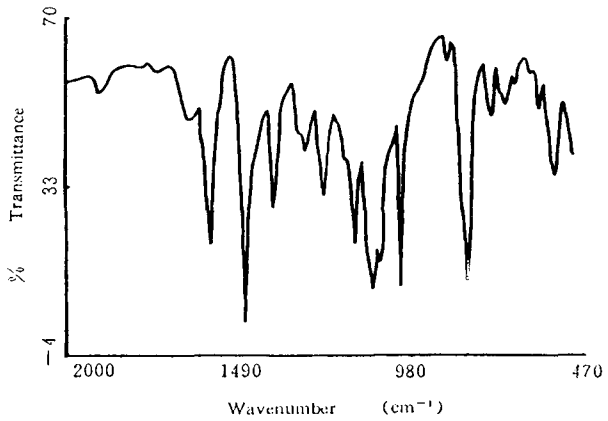

Figure 1 Infrared spectrum of the PPS–PES block copolymer.

—CH_2 absorption (1388 cm^{-1}) was selected as the reference analysis band, and C—O—C absorption (1242 cm^{-1}), as the quantitative analysis band. Then, the compositions of the PPS–PES block copolymers were analyzed quantitatively, and, furthermore, the weight percentage of PES in the copolymers was calculated through the standardized working curve (absorbance – PES weight).

Solubility Test

Ten milligram products were put into a test tube fitted with 10 mL solvent, stirred, and heated. Then the dissolution process and the result were observed.

X-ray Diffraction

X-ray diffraction spectra were obtained on a Rigaku Model 3014 X-ray diffractometer.

Thermal Analysis

Differential scanning calorimetric (DSC) and thermogravimetric (TG) data were measured on a Perkin-Elmer 7 series DSC and a DuPont 1090 TGA with heating rates of 20 and 10°C/min, respectively. The nonisothermal crystallization kinetics and thermal kinetics of PPS–PES block copolymers were

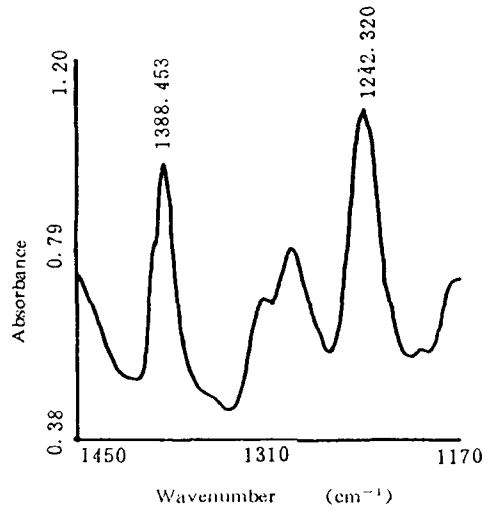

Figure 2 Quantitative analysis band 1242 cm^{-1} (C—O—C) and reference analysis band 1388 cm^{-1} (CH_2).

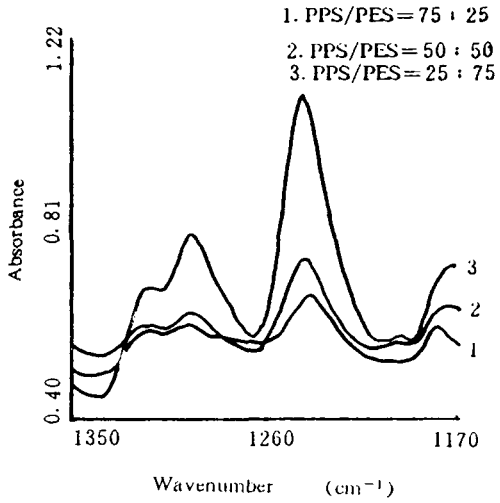

Figure 3 Relative absorption heights at different PPS/PES weight ratios.

studied by a Perkin-Elmer 7 series DSC and TGA. In the nonisothermal crystallization experiment, the polymer sample was cooled at rates of 5, 10, 15, and 20°C/min, and in the thermal decomposition experiment, the sample was heated at rates of 5, 10, and 15°C/min.

RESULTS AND DISCUSSION

Figure 1 shows the IR spectrum of the copolymer which reveals only peaks ascribable to absorptions of PPS and PES. There are absorption peaks at 1090 cm^{-1} for C—S, 1150 cm^{-1} for

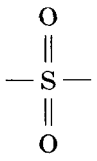

and 1240 cm^{-1} for C—O—C, etc. Figure 2 presents the quantitative analysis band and reference analysis band. The relative absorption heights of the above two bands under different PPS/PES weight ratios are shown in Figure 3. With the increasing of PES content in the copolymer, the vibration of C—O—C strengthens; hence, its absorption height increases.

The composition analytical results by coarse quantitative analysis and quantitative analysis are listed in Table I. It is found that the contents of PES in copolymers increase with the amount of PES in the added materials; however, the quantities of PES contents in copolymers are lower than in the feed. This can be explained by the following reasons: The PPS/PES weight ratio is not an optimal molar ratio; the reactivity of endgroups is not very high; and by the effects of reaction factors.[11,14]

Table II lists the solubilities of PPS–PES block copolymers. These soluble differences can be attributed to the reflection of different chain segments. Because α-chloronaphthalene is a good solvent for PPS and PES, the whole PPS–PES molecular chain is uncoiled in it, so the solution is homogeneous and transparent. But *m*-cresol is only a good solvent for PES; the PPS segment is a collapsed coil in it. Therefore, PPS chain segments of different molecular chains in *m*-cresol may be collected to form an insoluble zone and can become scattering particles of light, thus making the solutions appear white turbid.

The "white turbid" phenomenon can be described by Ceresa's model of the copolymer structure.[15] The molecular shape of copolymer in *m*-cresol is shown in Scheme II.

It can also be seen from Table II that with the increment of PES weight in the copolymer the solubility of the copolymer can be improved. For example, in NMP, there are suspended particles in

Table I Quantitative Analysis of Copolymer Compositions

No.	PPS/PES Oligomers Weight Ratio	Relative Intensity Ratio of Peak Height	Relative Intensity Ratio of Peak Area	Quantities of PES in Copolymer (*W* %)[14]
1[a]	75 : 25	0.3336	0.3870	6.3
2	50 : 50	0.5984	0.7550	15.5
3	25 : 75	0.9197	1.1834	24.8
1#[b]	75 : 25	0.2138	0.3181	5.3
2#	50 : 50	0.6470	0.8400	16.2
3#	25 : 75	0.6882	0.8972	18.6

[a] η_{inh} of PES oligomer is 0.25.
[b] η_{inh} of PES oligomer is 0.22.

solution 1* at 80°C, solution 2* appears "white turbid" at 40°C, but solution 3* is transparent at that temperature. It is concluded that the incorporation of the PES segment into the copolymer can improve the solubility of PPS.

The X-ray diffraction patterns of PPS–PES block copolymers are shown in Figure 4. The PPS segment can form a crystal phase by itself in block copolymers and the latter's crystal diffraction peaks (2θ values) are the same as those of pure PPS. Moreover, with the increment of PES weight in the copolymers, the crystal diffraction peaks weaken gradually. This result can also be proved by the DSC data.

The crystallinity of the copolymer (X_c) by DSC data and the crystallinity of the PPS constituent in copolymer (X'_c) can be calculated by the formula

$$X_c = \Delta H/\Delta H_f,\ X'_c = X_c/W_{\mathrm{PPS}}$$

where ΔH is the melting heat function of the copolymer; ΔH_f, the heat function of 100% crystalline PPS; ΔH_f = 112 J/g (Ref. 16); and W_{PPS}, the PPS weight percentage in the copolymer.

Table III lists the crystallinities of the block copolymers. With increase of the PES weight percentage in the copolymer, X_c reduces from sample 1 to sample 3. The X_c and X'_c drop by 8 and 6%, respectively, although the PES content in sample 1 is only 6.3%. It is proved that the incorporation of the PES segment into the PPS chain exerts an effect on the PPS crystalline ability, because with the increment of PES content in copolymer, the check and hinder action of the PES segment on the PPS segment enhances and that causes the reduction of the PPS crystalline ability.

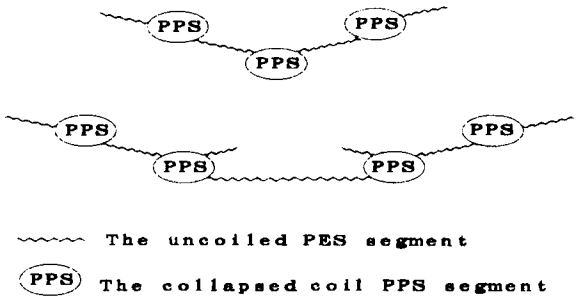

Scheme II The molecular shape of copolymer in *m*-cresol.

The DSC thermogram of the block copolymer is shown in Figure 5. From the thermogram and magnified part curve, the melting point temperature (T_m) and glass transition temperature (T_g) are obtained. The results are listed in Table IV. The T_{g_1} of samples 1 and 3 are higher than that of PPS (85°C), but the T_{g_2} lower than that of PES (225°C). It illustrates that the two samples are at phase-separating state although there is certain compatibility in the microphases. From the DSC data of sample 2, there is only one T_g and its value (141.4°C) is between that of PPS and PES. It shows that the copolymer is at a compatible state in this constitution range.

Figure 6 is a TG curve of block copolymer (sample 2). The initial and maximum decomposition temperatures are found to be 496.9 and 549.8°C, respectively. It is primarily proved that the PPS–PES block copolymer has good heat stability.

An attempt was made to apply the nonisothermal formalism developed by Ozawa[17] to PPS–PES crystallization exotherm data obtained at various rates

Table II Solubities of PPS–PES Block Copolymers

		No.		
Solvents	Temperature	1 PPS : PES = 75/25 PES % = 6.3%	2 PPS : PES = 50/50 PES % = 15.5%	3 PPS : PES = 25/75 PES % = 24.8%
DMF	T_b[a]	–[b]	–	–
DMAc	T_b	–	–	–
m-Cresol	T_b	Turbid	Turbid	Coagulation
Phenol/1,1,2,2-tetrachloroethane[c]	T_b	Turbid	Turbid	Coagulation
NMP	80°C	Turbid	Coagulation	+
α-Chloronaphthalene	Δ	+	+	+

[a] T_b means the boiling point; "Δ" means heating.
[b] "–" insoluble; "+" soluble.
[c] Phenol : 1,1,2,2-Tetrachloroethane = 2 : 3 (wt).

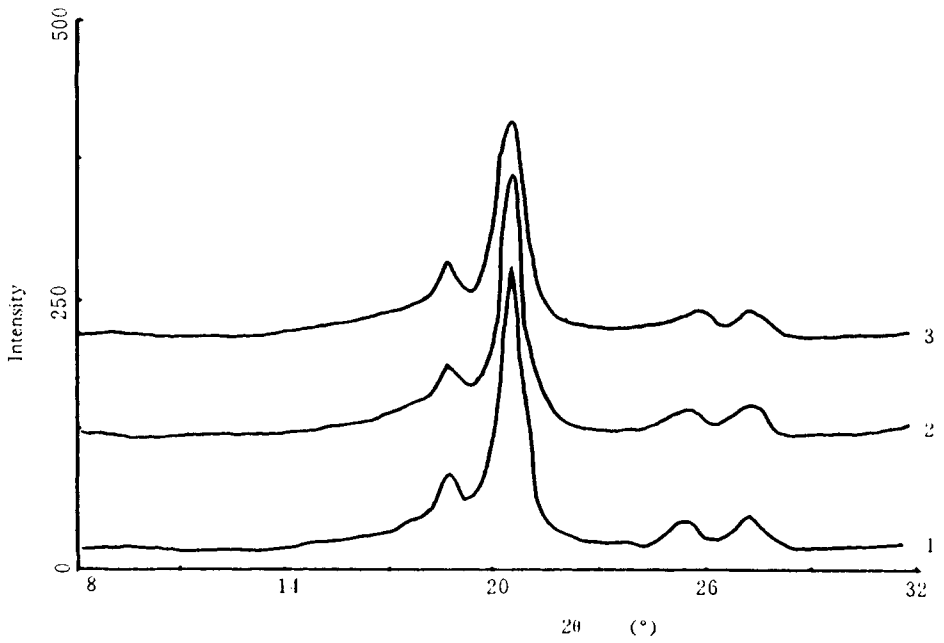

Figure 4 X-ray diffraction patterns of PPS–PES block copolymers.

of cooling.[18] By this method, the $\ln[-\ln(1 - Cr)]$ is plotted vs the ln (cooling rate) which represents the linearization of the following equation:

$$1 - Cr = \exp[-F(T)/\text{rate}^n] \qquad (1)$$

where Cr is the fraction of crystalline conversion; $F(T)$, the temperature-dependent parameter; and "rate," the cooling rate.

As to the constant cooling process, the $F(T)$ above is

$$F(T) = \left[-\frac{1}{n}\int_{T_0}^{T} K(T)\,dT\right]^n \qquad (2)$$

where $K(T)$ is the crystalline rate constant.

The nonisothermal Avrami calculations were worked on data that were digitized from the cooling curves obtained from the Perkin-Elmer 7 DSC.[19] The calculation uses Cr based on eq. (1) at each temperature for each cooling rate. Figure 7 shows the relative fraction of crystalline conversion $(1 - Cr)$ vs. temperature. Nonisothermal Avrami plots are shown in Figure 8; the slope of the lines is $-n$, and the intercept is $\ln F(T)$ from eq. (1).

Figure 9 describes the relationship of $\ln F(T)$ with temperature. From it, we can see that the two are in lines. The linear regression equation of the copolymer is shown below:

Table III Crystallinities of PPS–PES Copolymers

No.	PES (W %)	ΔH	X_c	X_c'
PPS-PES 1	6.3	47.0	42.0	44.8
PPS-PES 2	15.5	32.3	28.8	34.1
PPS-PES 3	24.8	20.2	18.0	23.9
PPS		56.5	50.4	50.4

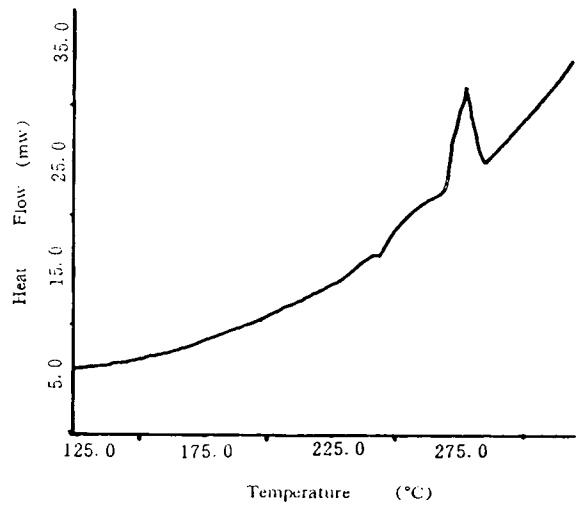

Figure 5 DSC curve of PPS–PES 2#.

Table IV DSC Data of PPS–PES Copolymers

No.	T_m (°C)	T_{g_1} (°C)	T_{g_2} (°C)
PPS–PES 1#	285.4	115.9	191.5
PPS–PES 2#	278.3	141.4	
PPS–PES 3#	283.8	119.6	198.7

$$\ln F(T) = aT + b = -0.21T + 47.63 \quad (3)$$

Put eq. (3) into eq. (2); the crystalline rate constant $K(T)$ is then

$$K(T) = -a \exp[(aT + b)/n]$$
$$= -0.21 \exp[(-0.21T + 47.63)/n] \quad (4)$$

Then, the half-life period of crystallization $t_{1/2}$ can be calculated by the Avrami equation $K = [(\ln 2)/(t_{1/2})^n]$. The data are listed altogether in Table V.

It is concluded from Table V that the crystalline rate decreases with the increment of temperature and the Avrami exponent n is about 1. This may be explained that as amorphous PES contents are incorporated into block copolymer the development of PPS crystal in the copolymer is hindered from every direction, and, thus, the crystallization becomes incomplete, so that the Avrami exponent n is less than that of normal PPS.

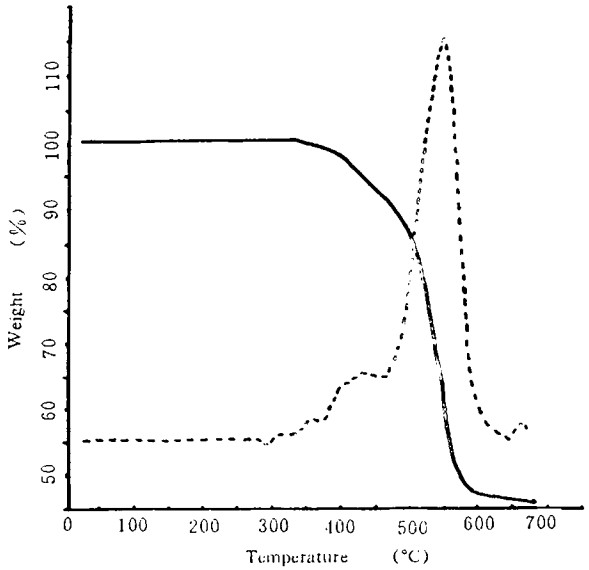

Figure 6 TGA curve of PPS–PES 2#.

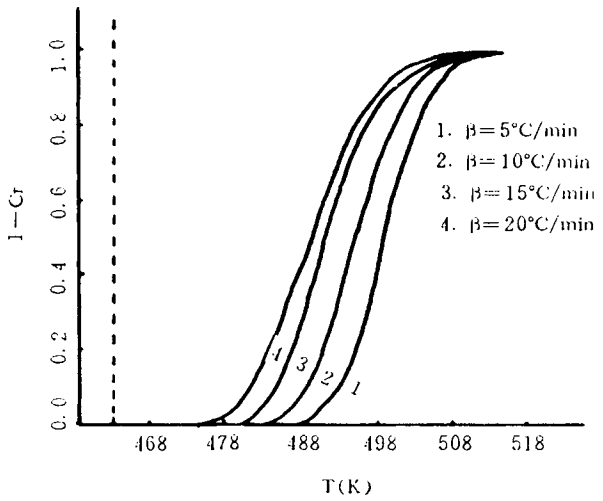

Figure 7 Crystallization curves at different cooling rates.

For the thermal decomposition process, the rate equation can be expressed as the following:

$$dw/dt = k(W - W_\alpha)^n \quad (5)$$

based on the Arrhenius equation:

$$k = Ae^{-E/RT} \quad (6)$$

and the heating rate $\beta = dT/dt$, so that eq. (6) can be written as below:

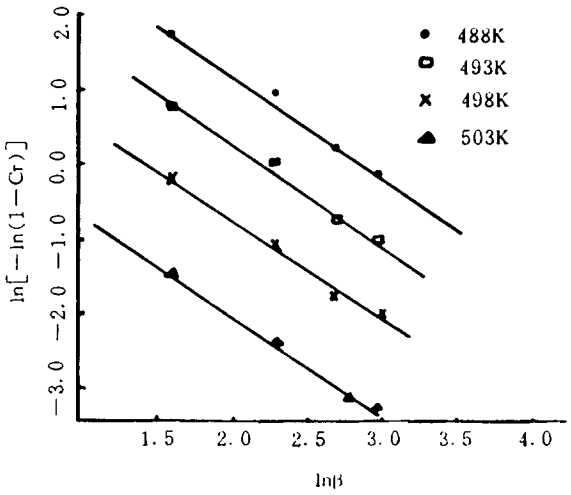

Figure 8 Plot of $\ln[-\ln(1 - Cr)]$ vs. $\ln \beta$ at different temperatures.

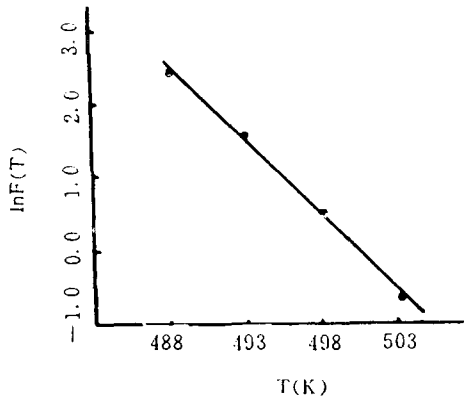

Figure 9 Plot of ln $F(T)$ vs. temperature.

$$dw/dT = [A/\beta][\exp(-E/RT)](W - W_\infty)^n \quad (7)$$

where n is reaction order, A, the preexponential factor of decomposition (s^{-1}); E, the activation energy of decomposition (J/mol); R, the gas constant (8.314 J/mol·k); W, the residual amount of decomposition at time t; and W_∞, the residual amount after complete decomposition.

Equation (7) can be changed as

$$\lg \beta = \lg \frac{AE}{R(W - W_\infty)^n} - 2.315 - 0.457 \frac{E}{RT} \quad (8)$$

From the TG curves, the temperatures corresponding to different decomposition fractions as 20, 30, and 40% are known (listed in Table VI). Figure 10 shows the plot of lg β vs. $1/T$. There seems to be three lines which are nearly parallel to each other. The activation energy of thermal decomposition is 187.3 kJ/mol from the average slope. So the PPS-PES block copolymer possesses good heat resistance.

Table V Kinetic Parameters of Nonisothermal Crystallization in PPS-PES Copolymer

No.	T (°C)	n	K (min^{-1})	$t_{1/2}$ (min)
1	215	1.3	1.415	0.578
2	220	1.3	0.631	1.075
3	225	1.3	0.281	2.003
4	230	1.3	0.125	3.735

Table VI TGA Data of Thermal Decomposition Kinetics of PPS-PES Copolymer

		T (K)/10^3 T^{-1} (K^{-1})		
β	lg β	20%	30%	40%
5	0.6990	771.8/1.296	790.9/1.264	803.8/1.244
10	1.0000	790.4/1.265	808.5/1.237	823.5/1.214
15	1.1761	802.4/1.246	820.1/1.219	836.1/1.196

CONCLUSION

The PPS-PES block copolymers have been prepared with chloro-terminated PPS oligomers and hydroxylic PES oligomers. Through FTIR spectroscopy, the contents of PES in the copolymer can be measured quantitatively and, hence, the compositions of block copolymers can be arranged. It has been furthermore proved that the block copolymers have better solubility, lower crystallinity, and higher T_g than has PPS alone. Through nonisothermal crystallization and thermal decomposition experiments, the crystallization kinetic parameters and the activation energy of thermal decomposition were calculated. It is shown that the crystalline rate decreases with the increment of temperature, and the Avrami exponent n is about 1 and the activation

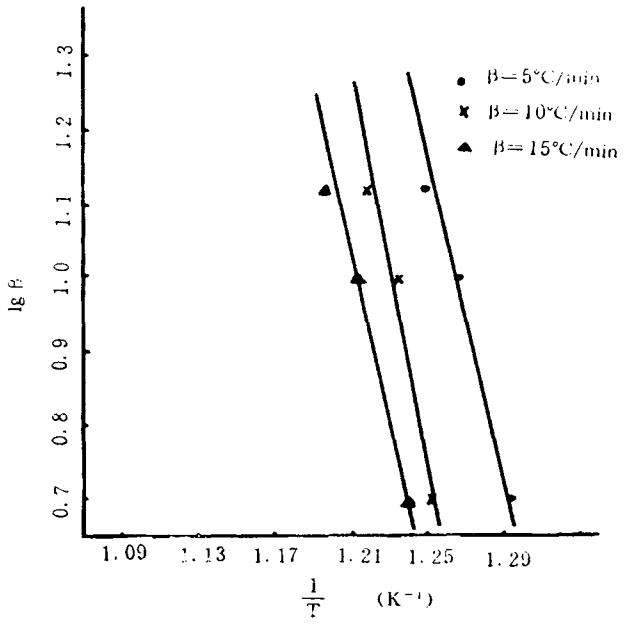

Figure 10 Plot of ln β vs. $1/T$.

energy of thermal decomposition is 187.3 kJ/mol. So, the PPS–PES block copolymers have good heat resistance.

This work was supported by the National High Technology Foundation of China.

REFERENCES

1. T. Kawabata and T. Sugie, U.S. Pat. 4,734,470 (1988).
2. F. W. Bailey, U.S. Pat. 4,021,596 (1977).
3. W. Ebert, K. Reuter, K. J. Idel, S. Kern, and G. Weymans, DE Pat. 3,900,916 (1989).
4. T. Kawabata, T. Sugie, F. Kobata, and A. Hirayama, U.S. Pat. 4,678,831 (1987).
5. K. Reuter, W. Ebert, and G. Weymans, DE Pat. 3,937,753 (1989).
6. L. Freund and W. Heitz, *Makromol. Chem.*, **191,** 815 (1990).
7. J. P. Blackwell and W. H. Beever, U.S. Pat. 4,703,081 (1987).
8. D. M. Teegarden, U.S. Pat. 4,997,894 (1991).
9. M. D. Herd and L. R. Kallenbach, U.S. Pat. 5,147,719 (1992).
10. Y. Kawakami, M. Hoshino, and Y. Satake, Eur. Pat. 459,620 (1991).
11. L. Kuang, Q. X. Wu, Z. L. Yu, and Y. R. Chen, *Suliao Gongye (Chin.),* **23**(6), 3 (1995).
12. L. Kuang, Q. X. Wu, Y. R. Chen, and Z. L. Yu, *Eur. Polym. J.*, to appear.
13. G. X. Miao, L. Kuang, Z. L. Yu, Y. R. Chen, and Q. X. Wu, *Suliao Gongye (Chin.),* **23**(3), 24 (1995).
14. L. Kuang, Q. X. Wu, Y. R. Chen, and P. Li, *Gaofenzi Cailiao Kexue Gongcheng (Chin.),* to appear.
15. J. R. Ceresa, *J. Polym. Sci. Part C Polym. Lett.*, **26,** 201 (1969).
16. P. Huo and P. Cebe, *Mater. Res. Soc. Symp. Proc.*, **93,** 215 (1991).
17. T. Ozawa, *Polymer,* **12,** 150 (1971).
18. G. L. Collins and J. D. Menczel, *Polym. Eng. Sci.*, **32,** 1270 (1992).
19. Z. Y. Zhang, *Gaofengzi Tongbao (Chin.),* **3,** 167 (1994).

Received September 9, 1995
Accepted March 30, 1996